

## **Glutaminolysis and lipoproteins are key factors in late immune recovery in successfully treated HIV-infected patients**

Isaac Rosado-Sánchez<sup>1±</sup>, Esther Rodríguez-Gallego<sup>2±</sup>, Joaquim Peraire<sup>2</sup>, Consuelo Viladés<sup>2</sup>, Pol Herrero<sup>3</sup>, Fran Fanjul<sup>4</sup>, Félix Gutiérrez<sup>5</sup>, Enrique Bernal<sup>6</sup>, Ricardo Pelazas<sup>7</sup>, Manuel Leal<sup>1,8</sup>, Sergi Veloso<sup>2</sup>, Miguel López-Dupla<sup>2</sup>, Julià Blanco<sup>9,10</sup>, Francesc Vidal<sup>2#\*</sup>, Yolanda María Pacheco<sup>1#\*</sup>, Anna Rull<sup>2#\*</sup>

<sup>1</sup> Laboratory of Immunology, Institute of Biomedicine of Seville, IBiS, UGC Clinical Laboratories, Virgen del Rocío University Hospital/CSIC/University of Seville, Seville, Spain

<sup>2</sup> Hospital Universitari Joan XXIII, IISPV, Universitat Rovira i Virgili, Tarragona, Spain

<sup>3</sup> Eurecat, Centre Tecnològic de Catalunya, Unitat de Ciències Òmiques (Unitat Mixta de Eurecat-Universitat Rovira i Virgili), Infraestructura Científico-Tècnica Singular (ICTS), Reus, Spain.

<sup>4</sup> Department of Infectious Diseases, Hospital Universitario Son Espases, Palma de Mallorca, Illes Balears, Spain

<sup>5</sup> Infectious Diseases Unit, Hospital General de Elche and Universidad Miguel Hernández, Alicante, Spain

<sup>6</sup> Department of Clinical Medicine, Universidad Católica San Antonio de Murcia and Hospital General Universitario Reina Sofía, Spain.

<sup>7</sup> Servicio de Medicina Interna, Hospital Universitario de Canarias, Universidad de La Laguna, Tenerife, Spain

<sup>8</sup> Internal Medicine Service, Viamed-Santa Ángela de la Cruz Hospital, Seville, Spain

<sup>9</sup> AIDS Research Institute IrsiCaixa, Institut Germans Trias i Pujol (IGTP); Universitat Autònoma de Barcelona, Badalona, Spain.

<sup>10</sup> Universitat de Vic-Universitat Central de Catalunya, Vic, Spain.

<sup>±</sup> Contributed equally to this work

<sup>#</sup> Senior authors that contributed equally to this work

\***Correspondence:** Francesc Vidal ([fvidalmarsal.hj23.ics@gencat.cat](mailto:fvidalmarsal.hj23.ics@gencat.cat)) or Yolanda M Pacheco ([ypacheco-ibis@us.es](mailto:ypacheco-ibis@us.es)) or Anna Rull ([anna.rull@iispv.cat](mailto:anna.rull@iispv.cat)).

## ABSTRACT

The immunological, biochemical and molecular mechanisms associated with poor immune recovery are far from known, and metabolomic profiling offers additional value to traditional soluble markers. Here, we present novel and relevant data that could contribute to better understanding of the molecular mechanisms preceding a discordant response and HIV progression under suppressive cART. Integrated data from NMR-based lipoprotein profiles, MS-based metabolomics and soluble plasma biomarkers help to build prognostic and immunological progression tools that enable the differentiation of HIV-infected subjects based on their immune recovery status after 96 weeks of suppressive cART. The metabolomic signature of ART-naïve HIV subjects with a subsequent late immune recovery is the expression of pro-inflammatory molecules and glutaminolysis, which is likely related to elevated T-cell turnover in these patients. The knowledge about how these metabolic pathways are interconnected and regulated provides new targets for future therapeutic interventions not only in HIV infection but also in other metabolic disorders such as human cancers where glutaminolysis is the alternative pathway for energy production in tumor cells to meet their requirement of rapid proliferation.

**Keywords:** Apoptosis, CD4<sup>+</sup> T-cell turnover, HIV, Inflammation, NMR-based lipoprotein profile, MS-based metabolomics, Poor immune recovery

## CLINICAL PERSPECTIVES

- Immunological non-responders are associated with worse long-term prognosis, including a higher risk of progression towards AIDS and non-AIDS-defining clinical events and death. Metabolomics profiling offers an additional value to traditional soluble markers.
- Here, we show novel and relevant data that corroborate our previous observation that inflammation and CD4<sup>+</sup> T-cell turnover are strongly linked in immune recovery.
- The metabolomic signature of ART-naïve HIV subjects with a subsequent late immune recovery is the expression of pro-inflammatory molecules and glutaminolysis. The knowledge about how these metabolic pathways are interconnected and regulated provides new targets for future therapeutic interventions not only in HIV infection but also in other metabolic disorders such as human cancers.

## **ABBREVIATIONS LIST**

cART, combined antiretroviral therapy  
CNTFR, ciliary neurotrophic factor receptor  
COS, Centre for Omic Sciences  
FDR, false discovery rate  
HCV, hepatitis C virus coinfection  
HDL, high-density lipoprotein  
HIF-1, hypoxia-inducible factor 1  
HMDB, human Metabolome Database  
hsCRP, high-sensitivity C-reactive protein  
IBD, inflammatory bowel disease  
IL-6, interleukin 6  
INR, immunological non-responders  
IP-10, interferon gamma-induced protein 10  
IR, immunological responders  
KW, Kruskal-Wallis  
LDL, low-density lipoprotein  
LPS, lipopolysaccharide  
MDA, mean decrease in accuracy  
MS, mass spectrometry  
MW, Mann-Whitney  
NAFLD, non-alcoholic fatty liver disease  
NMR, nuclear magnetic resonance  
PalC, palmitoylcarnitine  
PLS-DA, partial least squares discriminant analysis  
RF, random forest  
sCD14, soluble CD14  
sCD40L, soluble CD40 ligand  
sICAM-1, soluble intercellular adhesion molecules  
STITCH, Search Tool for Interactions of Chemicals  
sVCAM-1, soluble vascular cell adhesion molecule  
TGF- $\beta$ , transforming growth factor-beta  
TH, tyrosine hydroxylase  
VLDL- very-low density lipoprotein  
W, Wilcoxon t-test

## INTRODUCTION

Combined antiretroviral therapy (cART) successfully controls HIV viremia and improves the prognosis of HIV-infected subjects due to the decrease of HIV replication below detectable levels and due to CD4 T-cell recovery [1]. However, up to one fourth of HIV-infected subjects who start cART when they are severely immunosuppressed do not experience sufficient CD4 T-cell increases after two years of successful viral suppression. They are so-called “patients with incomplete recovery or discordant response”, “immunological non-responders (INR)” or “poor responders” [2–4]. In addition, although the concept of a poor immune response remains vague and the prevalence of INR varies between 10%-40% depending on the cohort studied [4–8], it is well established that patients receiving cART with CD4<sup>+</sup> T-cell counts persistently below 250 cells/ $\mu$ l are associated with worse long-term prognosis, including a higher risk of progression towards AIDS and non-AIDS-defining clinical events and death [9–11].

Previously, our group has retrospectively investigated the immune characteristics preceding poor CD4 recovery during cART in a cohort of INR patients. Increased expression of CD4 T-cell turnover-related markers (ki67/CD95) denoted an increased cycling and proliferative status in INRs before cART onset [12]. This phenomenon, together with an early profound immune dysregulation affecting Treg and Th17 cells [12,13], could contribute to the observed pro-inflammatory status that likely compromises the immune reconstitution of INR subjects. However, the integrated immunological, biochemical and molecular mechanisms associated with poor immune recovery are far from known. Investigations regarding the biologic mechanisms associated with this condition are needed to develop a useful tool for early detection of potential poor responders in daily clinical care and to investigate potential therapeutic targets.

The use of nuclear magnetic resonance (NMR) and mass spectrometry (MS) allows for the fast and reproducible quantification of several molecules simultaneously, offering additional value to the standard methodologies for diagnosis or clinical prognosis in the study of HIV infection [14]. We and others have recently demonstrated that plasma metabolomics is a powerful tool to

monitor natural HIV evolution or the effect of treatment as well as the metabolic diseases and chronic inflammation associated with HIV infection [15–19]. Our previous studies revealed that NMR-based metabolomics is a powerful instrument to identify a baseline lipoprotein profile associated with poor immune recovery [15] and dyslipidemia development in HIV-infected patients [16]. Untargeted plasma metabolomics profiling linked lipid abnormalities to circulating markers of inflammation, microbial translocation and hepatic function in HIV-infected subjects with advanced disease on PI-based cART [17], whereas targeted metabolomics identified an increased rate of glycolysis in HIV-infected CD4<sup>+</sup> T-cells [18] and alterations in the catabolism of branched amino acids associated with disease progression [19].

Because our previous NMR-based metabolomics analyses helped to define a baseline metabolomic signature of HIV-infected subjects with low nadir [15], we hypothesized that the combination of NMR-based lipoprotein profile and MS-based metabolomics could help to elucidate the molecular mechanisms associated with the increased CD4 T-cell turnover and immune dysregulation preceding poor immune recovery in our previously characterized cohort of HIV subjects [12,13]. Thus, we searched for potential predictive metabolomics markers of a late immune response before cART onset and HIV progression associated with discordant response after cART. For this aim, we performed circulating NMR- and MS-based HIV plasma metabolomics in 41 cART-naïve HIV-infected subjects who were subsequently followed up for 96 weeks under cART.

## **METHODS**

### **Study design and participants**

The study included 41 HIV-infected subjects aged  $\geq 18$  years and naïve to ART drugs recruited from the cohort of the Spanish AIDS Research Network (CoRIS) [20], which is an open cohort, multicenter cohort of patients newly diagnosed with HIV infection in the hospital or treatment centre, over 13 years of age, and naïve to antiretroviral treatment. For this study, we analyzed two groups of pre-cART samples from HIV-positive subjects along with the main risk factors associated with immune discordance [12] kindly provided by the HIV Biobank integrated in the Spanish AIDS Research Network (RIS) [21]. The study subjects included patients who started cART with counts of  $< 200$  CD4 cells/ $\mu\text{l}$  but did not achieve more than 250 CD4 cells/ $\mu\text{l}$  after 96 weeks of suppressive treatment (INR subjects,  $n = 18$ ) and a control group of patients who had also started cART with  $< 200$  CD4 cells/ $\mu\text{l}$  but achieved more than 250 CD4 cells/ $\mu\text{l}$  under the same conditions (IR subjects,  $n = 23$ ). Available follow-up samples (INR subjects,  $n = 9$  and IR subjects,  $n = 8$ ) after 96 weeks under suppressive cART were also analyzed. During this period, patients were receiving a combination of two nucleoside reverse transcriptase inhibitors (NRTI) plus a non-nucleoside reverse transcriptase inhibitor (NNRTIs) and/or a protease inhibitor(s) (PI) or a combination of both. Only two patients of each group were exposed to zidovudine (AZT), a known highly toxic NRTI-containing regimen. Data collection included basic clinical background and demographic information, as well as CD4 cell count, HIV-1 RNA viral load measurements and AIDS-defining events. Regarding viral load determinations, at least four viral load determinations throughout that period were measured, and all of which had to be below 40 HIV RNA copies/mL, except for the first six months following treatment initiation, where higher values were allowed [12]. Patients taking lipid-lowering agents (such as statins, fibrates or ezetimibe), antidiabetic drugs (such as metformin, sulfonylureas, DDP-4 inhibitors or insulin and analogues), psychotropic drugs (including antipsychotics or antidepressants) and other drugs with several known metabolic effects were excluded. Additionally, a group of healthy HIV-uninfected ( $n=9$ ) volunteers, matched by gender (all male)

and age (43 [40-48] years), was also analyzed for reference values. This study was carried out in accordance with the recommendations of the Ethical and Scientific Committees from each participating institution. All subjects gave written informed consent in accordance with the World Medical Association Declaration of Helsinki.

### **Plasma soluble markers**

Markers of systemic inflammation [interleukin (IL)-6, high-sensitivity C-reactive protein (hsCRP)], immune activation or suppression [interferon gamma-induced protein (IP)-10, soluble CD14 (sCD14), transforming growth factor-beta (TGF- $\beta$ )], microbial translocation [lipopolysaccharide (LPS)], endothelial dysfunction [soluble intercellular adhesion molecules (sICAM-1) and soluble vascular cell adhesion molecule (sVCAM-1)], platelet activation [soluble CD40 ligand (sCD40L)] and coagulation (D-dimer) were analyzed as described elsewhere [12]. Previous pre-cART data from several individual soluble parameters were partially published in a previous study including some patients from the same cohort [12] whereas values achieved at 96 weeks of cART were exclusively of the present work.

### **NMR lipoprotein measurements**

All  $^1\text{H}$  NMR spectra were recorded at 310 K on a Bruker Avance III 600 spectrometer operating at a proton frequency of 600.20 MHz. Lipid concentrations (i.e., triglycerides and cholesterol), lipoprotein sizes, and particle numbers for VLDL (38.6–81.9 nm), LDL (18.9–26.5 nm), and HDL (7.8–11.5 nm) classes, as well as the particle numbers of nine subclasses, namely, large, medium, and small VLDL, LDL, and HDL (a total set of 26 variables) were measured in 2D spectra from diffusion-ordered NMR spectroscopy (DOSY) experiments using the Liposcale test [22]. Briefly, the cholesterol and triglyceride concentrations of the main lipoprotein fractions were predicted using partial least squares (PLS) regression models. Then, the methyl proton resonances of the lipids in lipoprotein particles were decomposed into nine Lorentzian functions representing nine lipoprotein sub-classes and the mean particle size of every main fraction was derived by averaging the NMR area of each fraction by its associated size. Finally,

we calculated the particle numbers of each lipoprotein main fraction by dividing the lipid volume by the particle volume of a given class and we used the relative areas of the lipoprotein components used to decompose the NMR spectra in order to derive the particle numbers of the nine lipoprotein subclasses.

### **Metabolomic analysis**

Metabolomic profiling was performed by the Centre for Omic Sciences (COS) (<http://omicscentre.com/>) using ultra-high-performance liquid chromatography coupled to quadrupole-time of flight high-resolution mass spectrometry (UHPLC-(ESI)qTOF) using positive and negative ionization and hydrophilic interaction liquid chromatography coupled to quadrupole-time of flight high-resolution mass spectrometry (UHPLC-(ESI)qTOF) using positive ionization. The instrument was an Agilent 1290 Infinity UHPLC coupled to 6550 i-funnel qTOF, and chromatographic columns were an Acquity UPLC® HSS T3 C18 (100 x 2.1 mm., 1.8 µm) for UHPLC positive ionization, an Acquity UPLC® BEH C18 (100 x 2.1 mm., 1.8 µm) for UHPLC negative ionization and an Acquity UPLC® BEH HILIC (100 x 2.1 mm., 1.7 µm) for HILIC positive ionization, all from Waters, USA. The chromatographic analyses were performed under gradient elution using ultrapure water (0.1% formic acid) and acetonitrile for the UHPLC positive ionization method, ultrapure water (1 mM ammonium fluoride) and acetonitrile for the UHPLC negative ionization method and ultrapure water (50 mM ammonium acetate) and acetonitrile for the HILIC positive ionization method. The flow rate was 0.4 mL/min, the column temperature was set at 25°C and the injection volume was 2 µL (+4°C) for all methods. The acquisition range was between 100-1000 m/z at 1.5 spectra/sec.

The extraction of plasma metabolites was conducted by protein precipitation using methanol:water (8:1). A total of 450 µL of extracting solution were added to 50 µL of serum and were mixed for 10 sec and sonicated for 2 min. Next, the solution was kept for 10 min on ice and then centrifuged at 15000 rpm at +4 °C. The remaining supernatants were transferred to LC vials for analysis.

For tentative identification of metabolites, Mass Profinder software (Agilent) was used for data deconvolution and Mass Profiler Professional (Agilent) was used for data alignment for all samples. The aligned features were submitted to the ID Browser module for identification by their exact mass and retention time using the Metlin Personal Compound Database (Agilent). A total of 99 metabolomic entities were initially identified, and pre-processing data analysis was performed to exclude variables with constant or single values. Missing values for a given metabolite were detected and replaced by the median value of the metabolite. Partial least squares discriminant analysis (PLS-DA) was performed in the Metaboanalyst web portal ([www.metaboanalyst.ca](http://www.metaboanalyst.ca)). Random Forest (RF) and hierarchical clustering of signature metabolites associated with immune recovery were performed using the R. Both, human Metabolome Database (HMDB) (<http://www.hmdb.ca/>) [23] and the MetabolomeXchange web portal (<http://www.metabolomexchange.org>) were used to confirm the presence of metabolites identified in the human body and to obtain detailed information about the metabolites found in our study.

### **Statistical Analysis**

The normality of the distribution of the variables was assessed using a Kolmogorov-Smirnov test. Medians and interquartile ranges or means and standard deviations were used to summarize the continuous variables, and comparisons between the groups were performed with non-parametric Kruskal-Wallis (KW) and/or Mann-Whitney (MW) tests for unpaired samples and a Wilcoxon t-test for paired samples (W). The categorical variables are summarized as frequencies and percentages, and their associations with immune recovery were determined using the  $\chi^2$  test. Spearman correlation coefficients and the corresponding *P* values were calculated to assess the associations between CD4 counts and the estimated plasma lipoprotein, metabolome and lipidome entities and soluble parameters. Random forest (RF) analyses were performed as multivariate tests to identify the variables that best partitioned the overall study population according to immune recovery predisposition. The RF interpretations are represented using the mean decrease in accuracy (MDA) variable, which estimates how much excluding (or

permuting) each variable reduces the accuracy of the model during the out-of-bag error calculation phase. The variables with large MDAs were selected, and logistic regression models that combined the statistically significant variables were generated in both univariate and multivariate tests. Statistical analyses were performed using SPSS (version 21.0, SPSS Inc., Chicago, IL) and the R software computing environment (<https://www.r-project.org/>). The graphical representations are based on both the graphical environment of R and GraphPad Prism software (version 5.0, GraphPad Inc., San Diego, CA). The metabolite-protein interaction network and functional enrichment analyses were generated using the Search Tool for Interactions of Chemicals (STITCH) database, version 5.0 [24]. The results were considered significant at  $P < 0.05$ .

## RESULTS

### Patient characteristics

Forty-one cART-naïve patients were included in the study. The baseline clinical characteristics of the HIV-infected subjects (n = 41) are presented in **Table 1**. All patients were male, with a median age of 42 (34-51) years, with low CD4 counts (86 [63-161] cells/ $\mu$ L) and plasma viral loads (4.86 [4.41-5.37] log HIV RNA copies/mL). Both the INR and the IR group had similar frequencies of HCV co-infection (7.5%) and AIDS-related illness (24.4%). Based on the classification criteria, after 96 weeks under suppressive cART, INR subjects achieved 210 [176-235] CD4 T-cells/ $\mu$ L and a CD4/CD8 T-cell ratio of 0.32 [0.23-0.41], whereas IR subjects achieved 436 [360-570] CD4 T-cells/ $\mu$ L and a CD4/CD8 T-cell ratio of 0.38 [0.31-0.48].

### Pre-cART profile of soluble biomarkers predicting poor immune recovery after ART

Lipoprotein profile, lipidome and metabolome entities were analyzed in order to characterize groups of study. Previous pre-cART data from several individual soluble parameters were also included in order to improve the prognostic value of the metabolomics signature [12]. As expected, among a selection of soluble biomarkers of inflammation, immune activation/suppression, microbial translocation, endothelial dysfunction, platelet activation and coagulation, only higher IL-6 levels and a greater number of subjects having hsCRP  $\geq$  5 mg/L were found in INR subjects compared to IR subjects (**Supplementary Table 1**). Additionally, whereas no differences were found regarding the baseline pre-cART Liposcale lipoprotein characterization (**Supplementary Table 2**), the metabolite PLS-DA score plot, including lipidomic markers, was different between INR subjects and IR subjects before cART onset (**Figure 1A**). In fact, univariate analysis revealed an elevated concentration of L-tyrosine and a decreased concentration of L-glutamate and phosphatidylcholine PC (16:1) at baseline associated with later poor immune recovery (**Figure 1B**).

Next, random forest analysis (RF) was used as a multivariate method to rank variables (integrated data) that constitute the best predictors of immune recovery (**Figure 1C**). In

particular, RF provided additional evidence indicating that IL-6 and PC (16:1) were among the most discriminatory parameters (MDA>30) between INR subjects and IR subjects before cART onset. Palmitoylcarnitine concentrations also had a strong classification power in the multivariate model despite not appearing to be significantly different in the univariate test (**Figure 1B**), and increased plasma hsCRP  $\geq 5$  mg/L was the best classifier (MDA > 58). We next evaluated which metabolic pathways were affected by the interaction of these selected metabolites and proteins (**Figure 2A**). Surprisingly, in the biological process category, microbial translocation was one of the most-enriched terms along with the expected inflammatory (IL-6) and acute-phase response (hsCRP), suggesting a connection between the expression of pro-inflammatory cytokines and microbial translocation in the discordant response (**Figure 2B**). Gene ontology of cellular component categories further confirmed the enrichment of IL-6 complex and T-cell complex, as well as, their connection to neuronal components (**Figure 2B**). Notably, ciliary neurotrophic factor receptor (CNTFR), which supports the survival of neurons, is closely related to IL-6 receptor. Thus, the enriched KEGG pathway revealed a strong relationship between pre-cART immune recovery not only with immune processes (hematopoietic cell lineage, Jak-STAT signaling pathway, T-cell receptor) but also with key regulatory factors of T-cell glycolysis (HIF-1 signaling pathways) inflammatory disorders (IBD, NALFD), and alanine, aspartate and glutamate metabolism (**Figure 2B**).

### **High density lipoproteins and glutamate metabolism are strongly associated with immune recovery after cART**

Next, we examined lipoprotein alterations and analyzed soluble parameter changes after suppressive cART therapy in a group of 17 HIV-infected subjects with available follow-up samples after 96 weeks on stable cART (**Supplementary Table 3**). INR subjects (n = 9) had increased HDL cholesterol and increased HDL particle sizes, mainly due to increased medium HDL-P, compared to IR subjects (n = 8) (**Figure 3A**). Regarding the soluble plasma markers,

INR subjects had reduced concentrations of transforming growth factor beta (TGF- $\beta$ ) after suppressive cART (**Figure 3A, Supplementary Table 4**).

Next, we also studied the effect of successful immune restoration on the HIV plasma metabolome and lipidome. A supervised two-dimensional PLS-DA score plot clearly distinguished INR subjects from IR subjects (**Figure 3B**). Univariate analysis revealed a significantly decreased concentration of 5-aminolevulinic acid, eicosapentaenoic acid, gamma-glu-leu, glycolic acid, isopimaric acid and L-glutamate in INR subjects compared to IR subjects (**Figure 3C**). In this case, RF ranked HDL-C, LDL-C, HDL-P, and L-glutamate as the top parameters accounting for immune recovery after cART (**Figure 3D**).

### **Correlation analyses between CD4<sup>+</sup> T-cell counts and metabolomics signature after cART**

Discordant response is clearly defined by CD4<sup>+</sup> T-cell counts after cART, so we performed Spearman correlation analysis to confirm and detect the relationship between metabolomics and CD4<sup>+</sup> T-recovery. Correlation analyses of integrated data showed significant direct association of glycocholic acid ( $\rho = 0.51$ ,  $P = 0.04$ ), isopimaric acid ( $\rho = 0.74$ ,  $P = 0.04$ ), and citrulline ( $\rho = 0.60$ ,  $P = 0.03$ ) to CD4 T-cell count achieved after 96 weeks of suppressive cART. By contrast, CD4 T-cell count was inversely correlated to DL-pipecolic acid ( $\rho = -0.94$ ,  $P < 0.01$ ) and microbial translocation (LPS,  $\rho = -0.61$ ,  $P = 0.03$ ). In fact, networking modeling confirmed the relationship between glutamate metabolism not only to 5-aminolevulinic acid, citrulline (0.02 [0.02-0.03] in INR-subjects and 0.03 [0.01-0.03] in IR-subjects) and DL-pipecolic acid (0.07 [0.07-0.07] in INR-subjects and 0.03 [0.02-0.03] in IR-subjects), but also to “TGF $\beta$  family” via interaction to CCR2-CCL2 and retinoic acid axis (**Figure 3E**).

### **Longitudinal evaluation of lipoprotein metabolism and plasma soluble parameters**

Plasma NMR-based lipoprotein values achieved at 96 weeks of cART in HIV-infected subjects were compared to a control group of healthy volunteers (H-subjects) (1012 [801-1164] CD4 T-cells/ $\mu$ L). INR subjects had increased LDL-C ( $\Delta$ LDL-C = 31%) and LDL-P ( $\Delta$ LDL-P = 28%),

although their values remained significantly lower compared to the control group (**Figure 4A**, **Supplementary Figure 1**). In contrast, IR subjects reached similar LDL-C ( $\Delta$ LDL-C = 19%) values and LDL-P ( $\Delta$ LDL-P = 18%) values as healthy subjects (**Figure 4A**). Regarding HDL metabolism, INR subjects suffered a surprising increase in HDL-C ( $\Delta$ HDL-C = 42%) and HDL-P ( $\Delta$ HDL-C = 12%), achieving comparable values to healthy subjects, whereas in IR subjects these parameters remained lower compared to the reference group ( $P = 0.03$  and  $P < 0.01$ , respectively), despite the same longitudinal increasing trend ( $\Delta$ HDL-C = 16% and  $\Delta$ HDL-C = 7%) (**Figure 4B**, **Supplementary Figure 1**).

Next, we explored longitudinal changes in plasma soluble parameters associated with immune recovery. Both groups experienced a decrease in soluble markers of immune activation (IP-10) and endothelial dysfunction (ICAM-1, VCAM-1), although the differences were only significant in INR subjects (**Supplementary Figure 2**). In contrast, markers of platelet activation (CD40L) were slightly increased after ART therapy, and again, differences were only significant in INR subjects.

### **Metabolite restoration in relation to immune recovery**

To simplify data analysis, pre-processing was performed to include metabolites that were significantly different throughout the follow-up in HIV-infected subjects and metabolites that were significantly different between healthy volunteers and HIV-infected subjects at 96 weeks of cART. By this approach, four metabolites were significantly altered throughout the follow-up in INR subjects, nine metabolites were significantly altered throughout the follow-up in IR subjects and eight metabolites were exclusively associated with HIV infection (**Supplementary Table 5**).

Hierarchical clustering of this set of 35 metabolites clearly distinguished HIV-infected subjects from H-subjects after 96 weeks of cART. Furthermore, hierarchical clustering clearly distinguished INR subjects from IR and healthy subjects, indicating an anomalous immune

response after suppressive cART. Notably, after cART, IR subjects had similar metabolomic signatures as non-HIV-infected healthy volunteers (**Figure 5**).

## DISCUSSION

Recently, we demonstrated NMR-based metabolomics as a powerful tool to identify dyslipidemia development in HIV-infected subjects [16] and a baseline lipoprotein profile associated with poor immune recovery [15]. Here, we show that integrated data from NMR-based lipoprotein profiles, MS-based metabolomics and soluble plasma biomarkers builds prognostic and immunological tools that allow the differentiation of HIV-infected subjects based on their immune recovery status after 96 weeks of stable cART. Inflammation, glutaminolysis and structural and compositional changes in lipoproteins were associated with late immune recovery in INR subjects with increased CD4 T-cell turnover and immunological dysregulation. To our knowledge, this is the first study to evaluate plasma predictive markers and disease progression using NMR and MS-based metabolomics along with traditional soluble markers in a longitudinal study of HIV-infected subjects initiating cART with a subsequent low CD4<sup>+</sup> T-cell counts (less than 200 cells/  $\mu$ l), and with followed up for 96 weeks of cART. The current study is consistent with our previous observation [12] that associated higher levels of IL-6/hsCRP and increased CD4<sup>+</sup> T-cell turnover (ki67/CD95 expression) in INRs before cART onset, and offers new insight about the metabolic pathways involved.

Plasma IL-6, hsCRP  $\geq$  5mg/L, L-tyrosine, L-glutamate and PC (16:1) by univariate model, and hsCRP, IL-6 and palmitoylcarnitine (PalC) by multivariate model (RF), were identified as predictive markers of late immune recovery. PalC is a long-chain acyl fatty acid ester of carnitine that has associated with decreased Treg cell number in *Salmonella* infection [25] due to apoptosis regulation and hence associated with pro-inflammatory effects on the immune response [26]. Consistent with this, increased plasma PalC and IL-6 concentrations, as well as a greater number of subjects having hsCRP  $\geq$  5mg/L, were the best classifiers of late poor immune recovery in the RF model. Accordingly, we have recently described increased levels of IL-6 and hsCRP preceding poor CD4 T-cell recovery [12]. For instance, IL-6 activates the STAT3 signaling pathway, boosting the upregulation of the Th17-promoting transcription factor ROR $\gamma$ t which is also directly induced by the transcription hypoxia-inducible factor 1 (HIF-1)

[27,28]. HIF-1 is a key metabolic sensor expressed in CD4<sup>+</sup> T-cells that regulates the Th17/Treg balance by upregulating glycolytic metabolism in a mTOR-dependent manner [29,30].

Consistent with this, our previous work also demonstrated that increased frequencies of Th17 cells precede the discordant response to cART, suggesting that immune dysregulation affecting these subsets is critical in immunological non-responders to cART and could be linked to their inflammatory state [13]. T-cell activation drastically increases the metabolic demands, downregulating the characteristic pathways of quiescent cells via the induction of the transcription factor Myc as well as HIF-1 via the PI3/Akt/mTOR and NF-κB pathways [27,31]. In effect, increased glycolytic metabolism was previously associated with low CD4<sup>+</sup> T-cell counts and abnormally high levels of immune activation due to metabolic depletion of CD4<sup>+</sup> T-cell counts in HIV subjects [32]. Additionally, expression of NF-κB is activated by PC turnover, and thus, PC breakdown assumes a major role in HIV replication [33]. Interestingly, HIV replication in INR subjects under suppressive cART may be related to the existence of a population of metabolically active CD4<sup>+</sup> OX40<sup>+</sup> T cells that are highly susceptible to HIV infection [34], and we recently observed that such a population was upregulated both before and after cART initiation in INR subjects [35]. Thus, according to our results, we suggest that cell cycle regulation and inflammatory molecules are tightly interrelated and could induce the activation of key regulatory factors of T-cell glycolysis in HIV patients with poor immune response before starting cART.

On the other hand, the increased concentrations of plasma L-tyrosine could also be related to increased CD4<sup>+</sup> T-cell activation and the production of pro-inflammatory cytokines in INR subjects [36,37]. L-tyrosine is a non-essential amino acid and a precursor of brain catecholamines (dopamine, norepinephrine and epinephrine), that could be produced by lymphocytes in an autocrine or paracrine fashion [38]. It is known that dopamine reduces the suppressive and trafficking activities of Treg cells via the ERK signaling pathway [36]. Additionally, overexpression of tyrosine hydroxylase (TH), the enzyme responsible for catalyzing the conversion of L-tyrosine to L-DOPA, facilitates a shift in T-helper cell

differentiation and function towards Th2 cells direction, promoting the production of anti-inflammatory cytokines [37]. Therefore, we could hypothesize that INR subjects have diminished TH activity, accumulating higher circulating plasma L-tyrosine and, as a consequence, increasing CD4<sup>+</sup> T-cell exhaustion and promoting a Th1/Th2 shift towards Th1 cells, which is also consistent with the excess of pro-inflammatory cytokines in patients with poor immune recovery.

We have recently reported increased expression of CD4 T-cell turnover-related markers (Ki67/CD95) in INR subjects before cART initiation [12]. Here, we observed that these high rates of cellular turnover likely maintain the L-glutamate concentration far from what can be offset even after 96 weeks of cART, which may be associated with damage of the gastrointestinal (GI) tract and microbial translocation. Our results revealed that CD4<sup>+</sup> T-cell count was positively correlated with glycocholic acid, a primary bile acid, and the concentration of citrulline, a biomarker of intestinal diseases and enterocyte function [39,40]. CD4<sup>+</sup> T-cell count was also inversely correlated with both LPS, a bacterial by-product already associated with higher glucose uptake in monocytes [41], and DL-pipecolic acid, a product of lysine degradation [42]. Thus, damage of the GI tract and microbial translocation could be associated with worse prognosis of immune recovery in patients receiving cART. In this context, L-glutamate is an ATP-producing substrate for enterocytes as well as a precursor for citrulline synthesis [39], which is also negatively influenced by hsCRP, likely due to HIV replication, with depletion of CD4<sup>+</sup> T-cells leading to enterocyte loss [40]. Bile acids directly impact the adaptive immune response via inhibition of Th1 activation via Vitamin D receptor (VDR) signaling [43]. Furthermore, D-Pipecolic acid is metabolized from lysine by intestinal bacteria, and their uptake into the mitochondria was related to the development of hepatic encephalopathy via the induction of apoptosis in neuronal cells [44]. Additionally, high levels of circulating LPS were previously related to elevated CD4<sup>+</sup> T-cell turnover, suggesting an increased translocation of microbial products through the gastrointestinal mucosa in HIV incomplete responders [45,46].

Both protein and lipid compositional changes in HDL particles were previously associated with structural and functional changes in these lipoproteins in HIV infection [47]. Here, we observed increased HDL metabolism (HDL-C and HDL-P) in INR subjects after 96 weeks of cART that was surprisingly even higher than in healthy volunteers. HDL particles are heterogeneous in their shape, size, and surface charge with diverse functionality. HDLs are known to be the principal mean to transport lipid from extrahepatic cells back to the liver for degradation or recycling, but growing evidence challenges the role of HDL and its components in glucose metabolism via a variety of mechanisms [48]. HDL activates Akt phosphorylation in ApoA-I transgenic mice enhancing both glycolysis and glucose oxidation in mouse muscle cells and facilitating glucose uptake through an ABCA1/AMPK-dependent mechanism. In addition, although it is well recognized that HDL exerts anti-inflammatory effects reducing the secretion of several cytokines and chemokines, recent evidence also suggests a clear pro-inflammatory effect of HDL on macrophages. Disruption of membrane lipid rafts by HDL action increases the production of pro-inflammatory cytokines via the NF- $\kappa$ B/STAT1-IRF1 axis [49]. Furthermore, increased HDL particles could be related to the downregulation of TGF- $\beta$ , which is critical for the suppression of Th1 cell differentiation. In vitro evidence suggests that HDL can decrease the TGF- $\beta$ 1-mediated induction of  $\alpha$ -smooth muscle actin expression and TGF- $\beta$ 1-induced collagen deposition in human aortic endothelial cells [50]. Consistent with these data, our results revealed decreased TGF- $\beta$  concentrations in INR subjects compared to IR subjects after 96 weeks of cART. Thus, taken together, our data suggest that substantial remodeling of up-regulated HDL particles contribute to combat lipid accumulation from the cell membrane components of apoptotic cells, skewing the Th1/Th2 balance towards Th1 cells and thus promoting an inflammatory status and enhancing the expression of key glycolysis genes in INR subjects.

Our study has some notable limitations. The number of patients per groups was relatively small, a phenomenon that is offset by the study design that makes the groups of study more comparable and also because the sample size in untargeted metabolomics is considered less

relevant than in other types of studies. Also, no standard definition for the immunological response is available and therefore the threshold of 250 of CD4<sup>+</sup> T-cells/ $\mu$ L could seem somewhat arbitrarily set for the present study. In this regard, we have previously validated that patients receiving cART with CD4<sup>+</sup> T-cell counts persistently below 250 cells/ $\mu$ L are poor immunological responders and are associated with worse clinical outcomes [10,12,15]. On the other hand, to avoid CD4<sup>+</sup> T-cells as a confounding factor, HIV-infected subjects were matched by pre-cART CD4<sup>+</sup> T cell count and other confounding factors, that making our results more consistent in the search of a predictive metabolomic signature. However, lower median values in INR subjects can be observed compared to IR subjects, probably due to the relevance of the CD4<sup>+</sup> T-cell count before cART onset as an intrinsic risk factor of immune failure to cART.

In conclusion, this study presents novel and relevant data that corroborate our previous observation that inflammation and CD4<sup>+</sup> T-cell turnover are strongly linked in this context [12] and contributes to a better understanding of the molecular mechanisms preceding a discordant response and immunological progression under suppressive cART. NMR and MS-based metabolomics can be prognostic immunological progression tools, and their combination with traditional soluble parameters increases the metabolomic biomarker value. The knowledge of how these metabolic pathways are interconnected and regulated provides new targets for future therapeutic interventions not only in HIV infection but also to other metabolic disorders.

Cell cycle regulation and T-cell turnover seem to promote the expression of pro-inflammatory molecules and downregulate the characteristic pathways of quiescent cells in favor of glutaminolysis in an attempt to offset the CD4<sup>+</sup> T-cell exhaustion in INR subjects even after 96 weeks of cART. A specifically reduced thymic output in INR subjects could be the driver for the high requirement of their profoundly depleted CD4 T-cells to consequently switch on glutaminolysis, an alternative pathway of rapid energy production previously related to the proliferation of tumor cells. Additionally, metabolomic profiling supports previous studies suggesting that damage of GI tract and microbial translocation are associated with poor immune recovery in HIV-infected subjects under suppressive cART and highlight the diverse

functionality of HDL particles, especially by their relation to glucose metabolism and the regulation of pro-inflammatory cytokines/chemokines in INR subjects.

### ***Acknowledgments***

This study would not have been possible without the collaboration of all the patients, medical and nurse staff, and data managers who have taken part in the project. The authors would like especially to thank Veronica Alba for her technical support, Montserrat Vargas and Alfonso J. Castellano for nursing support at the HIV Unit at Hospital Universitari Joan XXIII (Tarragona), and Lluís Gallart and Miriam Campos from IISPV-Biobank platform at Universitari Joan XXIII (Tarragona). We acknowledge the HIV BioBank integrated in the Spanish AIDS Research Network and collaborating Centres for the generous gifts of clinical samples used in this work. The HIV Biobank, integrated in the Spanish AIDS Research Network, is supported by Instituto de Salud Carlos III, Spanish Health Ministry (RD06/0006/0035, RD12/0017/0037 and RD16/0025/0019) as a part of the Plan National R+D+I and cofinanced by ISCIII- Subdirección General de Evaluación y el Fondo Europeo de Desarrollo Regional (FEDER). The RIS Cohort (CoRIS) is funded by Instituto de Salud Carlos III through the Red Temática de Investigación Cooperativa en SIDA (RIS C03/173, RD12/0017/0018 and RD16/0002/0006) as part of the Plan National R+D+I and cofinanced by ISCIII- Subdirección General de Evaluación y el Fondo Europeo de Desarrollo Regional (FEDER). Authors greatly appreciate the comments and criticisms of the anonymous reviewers that greatly helped to improve the manuscript.

### ***Declaration of interest***

All authors declare they do not have anything to disclose regarding conflict of interest with respect to this manuscript.

### ***Funding***

This work was supported by the Fondo de Investigación Sanitaria [PI10/02635, PI13/0796, PI16/00503, PI18/01216, PI19/01337]-ISCIII-FEDER; Programa de Suport als Grups de Recerca AGAUR (2014SGR250, 2017SGR948); Gilead Fellowship Program GLD14/293; The SPANISH AIDS Research Network [RD12/0017/0005, RD16/0025/0006, RD16/0025/0019]-ISCIII-FEDER (Spain), Agencia Estatal de Investigación (Acciones de carácter internacional

“Europa Investigación”; EUIN2017-89297) and Consejería de Economía, Innovación, Ciencia y Empleo, Junta de Andalucía (Proyecto de Investigación de Excelencia; CTS2593). FV is supported by a grants from the Programa de Intensificación de Investigadores (INT15/226)-ISCIII. YMP is supported by the Servicio Andaluz de Salud through Programa Nicolás Monardes (C-0013-2017). AR is supported by a grant from the Acció Instrumental d’incorporació de científics i tecnòlegs (PERIS SLT002/16/00101), Departament de Salut, Generalitat de Catalunya.

### **Author contributions**

All authors have seen and approved the submitted version of the manuscript. The authors contributions are as follows: experimental design (IR-S, ER-G, PH, AR) and intellectual guidance (JP, CV); recruitment of subjects (JP, CV, ML, SV, MLD, JB, FF, FG, EB, RP) and sample procurement (IR-S, ER-G); data collection (IR-S, ER-G, PH); data analysis and interpretation (IR-S, YMP, AR); manuscript preparation (IR-S, ER-G, YMP, AR). IR-S, ER-G, JB, FV, YMP and AR were responsible for the study design, data analysis, and article development. FV, YMP and AR reviewed and edited the manuscript.

## References

1. Hernando V, Alejos B, Monge S, Berenguer J, Anta L, Vinuesa D, et al. All-cause mortality in the cohorts of the Spanish AIDS Research Network (RIS) compared with the general population: 1997-2010. *BMC Infectious Diseases*. *BMC Infectious Diseases*; 2013;13:382.
2. Battegay M, Nüesch R, Hirschel B, Kaufmann GR. Immunological recovery and antiretroviral therapy in HIV-1 infection. *Lancet Infect Dis*. 2006;6:280–7.
3. Goicoechea M, Smith DM, Liu L, May S, Tenorio AR, Ignacio CC, et al. Determinants of CD4+ T cell recovery during suppressive antiretroviral therapy: Association of immune activation, T cell maturation markers, and cellular HIV-1 DNA. *J Infect Dis*. 2006;194:29–37.
4. Pacheco YM, Jarrín I, Del Amo J, Moreno S, Iribarren J a, Viciano P, et al. Risk factors, CD4 long-term evolution and mortality of HIV-infected patients who persistently maintain low CD4 counts, despite virological response to HAART. *Current HIV Research*. 2009;7:612–9.
5. May MT, Gompels M, Delpech V, Porter K, Orkin C, Kegg S, et al. Impact on life expectancy of HIV-1 positive individuals of CD4R cell count and viral load response to antiretroviral therapy. *AIDS*. 2014;28:1193–202.
6. Masiá M, Padilla S, Álvarez D, López JC, Santos I, Soriano V, et al. Risk, predictors, and mortality associated with non-AIDS events in newly diagnosed HIV-infected patients: Role of antiretroviral therapy. *AIDS*. 2013;27:181–9.
7. Gazzola L, Tincati C, Bellistri GM, d'Arminio Monforte A, Marchetti G. The Absence of CD4 + T Cell Count Recovery Despite Receipt of Virologically Suppressive Highly Active Antiretroviral Therapy: Clinical Risk, Immunological Gaps, and Therapeutic Options. *CID*. 2009;48:328–37.
8. Casotti JAS, Passos LN, Oliveira FJP, Cerutti C. Factors associated with paradoxical immune response to antiretroviral therapy in HIV infected patients: A case control study. *BMC Infectious Diseases*. *BioMed Central Ltd*; 2011;11:306.

9. Engsig FN, Zangerle R, Katsarou O, Dabis F, Reiss P, Gill J, et al. Long-term mortality in HIV-positive individuals virally suppressed for >3 years with incomplete CD4 recovery. *CID*. 2014;58:1312–21.
10. Pacheco YM, Jarrin I, Rosado I, Campins AA, Berenguer J, Iribarren JA, et al. Increased risk of non-AIDS-related events in HIV subjects with persistent low CD4 counts despite cART in the CoRIS cohort. *Antiviral Research*. Elsevier; 2015;117:69–74.
11. Cenderello G, De Maria A. Discordant responses to cART in HIV-1 patients in the era of high potency antiretroviral drugs: Clinical evaluation, classification, management prospects. *Expert Rev Anti Infect Ther*. 2016;14:29–40.
12. Rosado-Sánchez I, Jarrín I, Pozo-Balado MM, de Pablo-Bernal RS, Herrero-Fernández I, Alvarez-Ríos AI, et al. Higher levels of IL-6, CD4 turnover and Treg frequency are already present before cART in HIV-infected subjects with later low CD4 recovery. *Antiviral Research*. 2017;142:76–82.
13. Rosado-Sánchez I, Herrero-Fernández I, Tarancon-Diez L, Moreno S, Iribarren JA, Dalmau D, et al. Increased frequencies of Th17 cells and IL17a-producing regulatory T-cells preceding the immunodiscordant response to antiretroviral treatment. *J Infect*. Elsevier Ltd; 2018;76:86–92.
14. Sitole LJ, Williams AA, Meyer D. Metabonomic analysis of HIV-infected biofluids. *Mol BioSyst*. 2013;9:18–28.
15. Rodríguez-Gallego E, Gómez J, Pacheco YM, Peraire J, Viladés C, Beltrán-Debón R, et al. A baseline metabolomic signature is associated with immunological CD4+ T-cell recovery after 36 months of ART in HIV-infected patients. *AIDS*. 2018;32:565–73.
16. Rodríguez-Gallego E, Gómez J, Domigo P, Ferrando-Martínez S, Peraire J, Viladés C, et al. Circulating metabolomic profile can predict dyslipidemia in HIV patients undergoing antiretroviral therapy. *Atherosclerosis*. 2018;273:28–36.

17. Cassol E, Misra V, Holman A, Kamat A, Morgello S, Gabuzda D. Plasma metabolomics identifies lipid abnormalities linked to markers of inflammation, microbial translocation, and hepatic function in HIV patients receiving protease inhibitors. *BMC Infectious Diseases*. 2013;13:203.
18. Hollenbaugh JA, Munger J, Kim B. Metabolite profiles of human immunodeficiency virus infected CD4<sup>+</sup> T cells and macrophages using LC-MS/MS analysis. *Virology*. 2011;415:153–9.
19. Scarpelini B, Zanoni M, Sucupira MCA, Truong HHM, Janini LMR, Segurado IDC, et al. Plasma metabolomics biosignature according to HIV stage of infection, pace of disease progression, viremia level and immunological response to treatment. *PLoS ONE*. 2016;11:e0161920.
20. Caro-Murillo AM, Castilla J, Perez-Hoyos S, Miro JM, Podzamczar D, Rubio R, et al. Spanish cohort of naïve HIV-infected patients (CoRIS): Rationale, organization and initial results | Cohorte RIS de pacientes con infección por VIH sin tratamiento antirretroviral previo (CoRIS): Metodología y primeros resultados. *Enferm Infecc Microbiol Clin*. 2007;25:23–31.
21. García-Merino I, de las Cuevas N, Jiménez J, Gallego J, Gómez C, Prieto C, et al. The Spanish HIV BioBank: A model of cooperative HIV research. *Retrovirology*. 2009;6:27.
22. Mallol R, Amigó N, Rodríguez MA, Heras M, Vinaixa M, Plana N, et al. Liposcale: a novel advanced lipoprotein test based on 2D diffusion-ordered <sup>1</sup>H NMR spectroscopy. *J Lipid Res*. 2015;56:737–46.
23. Wishart DS, Jewison T, Guo AC, Wilson M, Knox C, Liu Y, et al. HMDB 3.0—The Human Metabolome Database in 2013. *Nucleic Acids Res*. 2013;41:D801–7.
24. Szklarczyk D, Santos A, von Mering C, Jensen LJ, Bork P, Kuhn M. STITCH 5: augmenting protein–chemical interaction networks with tissue and affinity data. *Nucleic Acids Research*. 2016;44:D380–4.
25. Hulme HE, Meikle LM, Wessel H, Strittmatter N, Swales J, Thomson C, et al. Mass

- spectrometry imaging identifies palmitoylcarnitine as an immunological mediator during Salmonella Typhimurium infection. *Sci Rep.* 2017;7:2786.
26. Mutomba MC, Yuan H, Konyavko M, Adachi S, Yokoyama CB, Esser V, et al. Regulation of the activity of caspases by -carnitine and palmitoylcarnitine. *FEBS Letters.* 2000;478:19–25.
27. Tao J-H, Barbi J, Pan F. Hypoxia-inducible factors in T lymphocyte differentiation and function. A Review in the Theme: Cellular Responses to Hypoxia. *Am J Physiol Cell Physiol.* 2015;309:C580–9.
28. Dang E V, Barbi J, Yang H, Jinasena D, Yu H, Bordman Z, et al. Control of TH 17/Treg Balance by Hypoxia-inducible Factor 1. *Cell.* 2011;146:772–84.
29. Shi LZ, Wang R, Huang G, Vogel P, Neale G, Green DR, et al. HIF1 $\alpha$ -dependent glycolytic pathway orchestrates a metabolic checkpoint for the differentiation of T H 17 and T reg cells. *J Exp Med.* 2011;208:1367–76.
30. Palmer CS, Hussain T, Duette G, Weller TJ, Ostrowski M, Sada-Ovalle I, et al. Regulators of Glucose Metabolism in CD4 + and CD8 + T Cells. *Int Rev Immunol.* 2016;35:477–88.
31. Gerriets VA, Rathmell JC. Metabolic pathways in T cell fate and function. *Trends Immunol.* Elsevier Ltd; 2012;33:168–73.
32. Palmer CS, Ostrowski M, Gouillou M, Tsai L, Yu D, Zhou J, et al. Increased glucose metabolic activity is associated with CD4+ T-cell activation and depletion during chronic HIV infection. *AIDS.* 2014;28:297–309.
33. Arenzana-Seisdedos F, Fernandez B, Dominguez I, Jacqué JM, Thomas D, Diaz-Meco MT, et al. Phosphatidylcholine hydrolysis activates NF-kappa B and increases human immunodeficiency virus replication in human monocytes and T lymphocytes. *J Virol.* 1993;67:6596–604.
34. Palmer CS, Duette GA, Wagner MCE, Henstridge DC, Saleh S, Pereira C, et al.

Metabolically active CD4<sup>+</sup> T cells expressing Glut1 and OX40 preferentially harbor HIV during in vitro infection. *FEBS Letters*. 2017;591:3319–32.

35. Rosado-Sánchez I, Herrero-Fernández I, Genebat M, Del Romero J, Riera M, Podzamczer D, et al. HIV-infected subjects with Poor CD4 T-cell recovery despite effective therapy express high levels of OX40 and  $\alpha 4\beta 7$  on CD4 T-cells prior therapy initiation. *Frontiers in Immunology*. 2018;9:1–6.

36. Kipnis J, Cardon M, Avidan H, Lewitus GM, Mordechay S, Rolls A, et al. Dopamine, through the Extracellular Signal-Regulated Kinase Pathway, Downregulates CD4<sup>+</sup>CD25<sup>+</sup> Regulatory T-Cell Activity: Implications for Neurodegeneration. *J Neurosci*. 2004;24:6133–43.

37. Huang H-W, Zuo C, Chen X, Peng Y-P, Qiu Y-H. Effect of tyrosine hydroxylase overexpression in lymphocytes on the differentiation and function of T helper cells. *Int J Mol Med*. 2016;38:635–42.

38. Bergquist J, Tarkowski A, Ekman R, Ewing A. Discovery of endogenous catecholamines in lymphocytes and evidence for catecholamine regulation of lymphocyte function via an autocrine loop. *Proc Natl Acad Sci USA*. 1994;91:12912–6.

39. Blachier F, Boutry C, Bos C, Tomé D. Metabolism and functions of L -glutamate in the epithelial cells of the small and large intestines. *Am J Clin Nutr*. 2009;90:814S–821S.

40. Crenn P, De Truchis P, Neveux N, Galpérine T, Cynober L, Melchior JC. Plasma citrulline is a biomarker of enterocyte mass and an indicator of parenteral nutrition in HIV-infected patients. *Am J Clin Nutr*. 2009;90:587–94.

41. Palmer CS, Anzinger JJ, Zhou J, Gouillou M, Landay A, Jaworowski A, et al. Glucose Transporter 1–Expressing Proinflammatory Monocytes Are Elevated in Combination Antiretroviral Therapy–Treated and Untreated HIV + Subjects. *J Immunol*. 2014;193:5595–603.

42. Fujita T, Hada T, Higashino K. Origin of D- and L-pipecolic acid in human physiological fluids: a study of the catabolic mechanism to pipecolic acid using the lysine loading test. *Clin*

Chim Acta. 1999;287:145–56.

43. Pols TWH, Puchner T, Korkmaz HI, Vos M, Soeters MR, De Vries CJM. Lithocholic acid controls adaptive immune responses by inhibition of Th1 activation through the Vitamin D receptor. PLoS ONE. 2017;12:e0176715.

44. Matsumoto S, Yamamoto S, Sai K, Maruo K, Adachi M, Saitoh M, et al. Pipecolic acid induces apoptosis in neuronal cells. Brain Research. 2003;980:179–84.

45. Merlini E, Bai F, Bellistri GM, Tincati C, d'Arminio Monforte A, Marchetti G. Evidence for polymicrobial flora translocating in peripheral blood of HIV-infected patients with poor immune response to antiretroviral therapy. PLoS ONE. 2011;6:e18580.

46. Marchetti G, Bellistri GM, Borghi E, Tincati C, Ferramosca S, La Francesca M, et al. Microbial translocation is associated with sustained failure in CD4+ T-cell reconstitution in HIV-infected patients on long-term highly active antiretroviral therapy. AIDS. 2008;22:2035–44.

47. Siegel MO, Borkowska AG, Dubrovsky L, Roth M, Welti R, Roberts AD, et al. HIV infection induces structural and functional changes in High Density Lipoproteins. Atherosclerosis. 2015;243:19–29.

48. Siebel AL, Heywood SE, Kingwell BA. HDL and glucose metabolism: Current evidence and therapeutic potential. Front Pharmacol. 2015;6:258.

49. van der Vorst EPC, Theodorou K, Wu Y, Hoeksema MA, Goossens P, Bursill CA, et al. High-Density Lipoproteins Exert Pro-inflammatory Effects on Macrophages via Passive Cholesterol Depletion and PKC-NF- $\kappa$ B/STAT1-IRF1 Signaling. Cell Metabolism. Elsevier Inc.; 2017;25:197–207.

50. Spillmann F, Miteva K, Pieske B, Tschöpe C, Van Linthout S. High-density lipoproteins reduce endothelial-to-mesenchymal transition. Arteriosclerosis, Thrombosis, and Vascular Biology. 2015;35:1774–7.



## Figure legends

### Figure 1. Baseline integrated data associated with poor immune recovery

(A) Two-dimensional PLS-DA score plot of metabolomics and lipidomics analyses distinguishes INR subjects (red dots) from IR subjects (green dots). (B) Entities (arbitrary units) that clearly distinguish INR subjects from IR subjects in the univariate test (Mann-Whitney U test). Data are presented as mean  $\pm$  SEM. (C) Plot shows the mean decrease accuracy (MDA) from Random Forest (RF) analysis, ranking variables (MDA > 5.5) according to their prognostic importance for immune recovery. dGMP, deoxyguanosine 5'-monophosphate; a.u., arbitrary units.

### Figure 2. Network interactions associated with baseline poor immune recovery

(A) Network of metabolite-protein interaction generated with the set of 35 parameters that constitute the best predictors of immune recovery according the Random Forest model. The names of the integrated data (soluble protein markers and metabolites) were used as input in the Search Tool for Interactions of Chemicals (STITCH) database. (B) The STITCH database identified different functional enrichments associated with our network using the false discovery rate (FDR). The strong biological process and KEGG pathways included the expected IL-6-mediated signaling pathways but also microbial translocation, inflammatory bowel disease (IBD) and glutamate metabolism, among others. CNTFR, ciliary neurotrophic factor receptor; NAFLD, non-alcoholic fatty liver disease. Glutamate metabolism refers to alanine, aspartate and glutamate metabolism.

### Figure 3. Plasma lipoprotein metabolism and metabolome associated with immune recovery after cART

(A) Plasma lipoprotein characteristics and TGF $\beta$  concentration associated with immune recovery after 96 weeks of cART. Data are presented as box and whiskers plots (min to max). (B) Two-dimensional PLS-DA scatter plot constructed with plasma metabolomic and lipidomic

entities clearly distinguishes IR subjects (green dots) from INR subjects (red dots). (C) Data presented as mean  $\pm$  SEM from metabolites differentially expressed between INR subjects from IR subjects in the univariate U-test. (D) Plot shows the mean decrease accuracy (MDA) from Random Forest analysis ranking parameters (MDA > 10) according to their prognostic importance for immune recovery. (E) The STITCH database illustrated the association between CD4, “glutamate” and “TGF- $\beta$  family” using the false discovery rate (FDR).

**Figure 4. Longitudinal evolution of the lipoprotein profile in a follow-up subgroup of 8 INR and 9 IR subjects in comparison with a group of healthy volunteers**

(A) Both, INR subjects and IR subjects exhibited increased LDL-C and LDL-P after 96 weeks of cART. Whereas INR subjects values remained significantly lower compared to the control group, IR subjects reached similar values to healthy volunteers (H-subjects). (B) HDL-C and HDL-P exhibited a surprising slight increase in INR subjects achieving comparable values to healthy subjects, but remained lower in IR subjects compared to healthy subjects. Comparisons between groups were performed with Mann-Whitney (MW) tests for unpaired samples and Wilcoxon t-test for paired samples (W). B was the abbreviation used for pre-cART values, and P was the abbreviation used for values after 96 weeks of cART.

**Figure 5. Hierarchical clustering of metabolites altered during cART**

(A) Hierarchical clustering of a set of 35 metabolites that were different throughout the follow-up in both groups of HIV patients and different between healthy volunteers and HIV-infected patients at 96 weeks of cART.

**Figure 1**

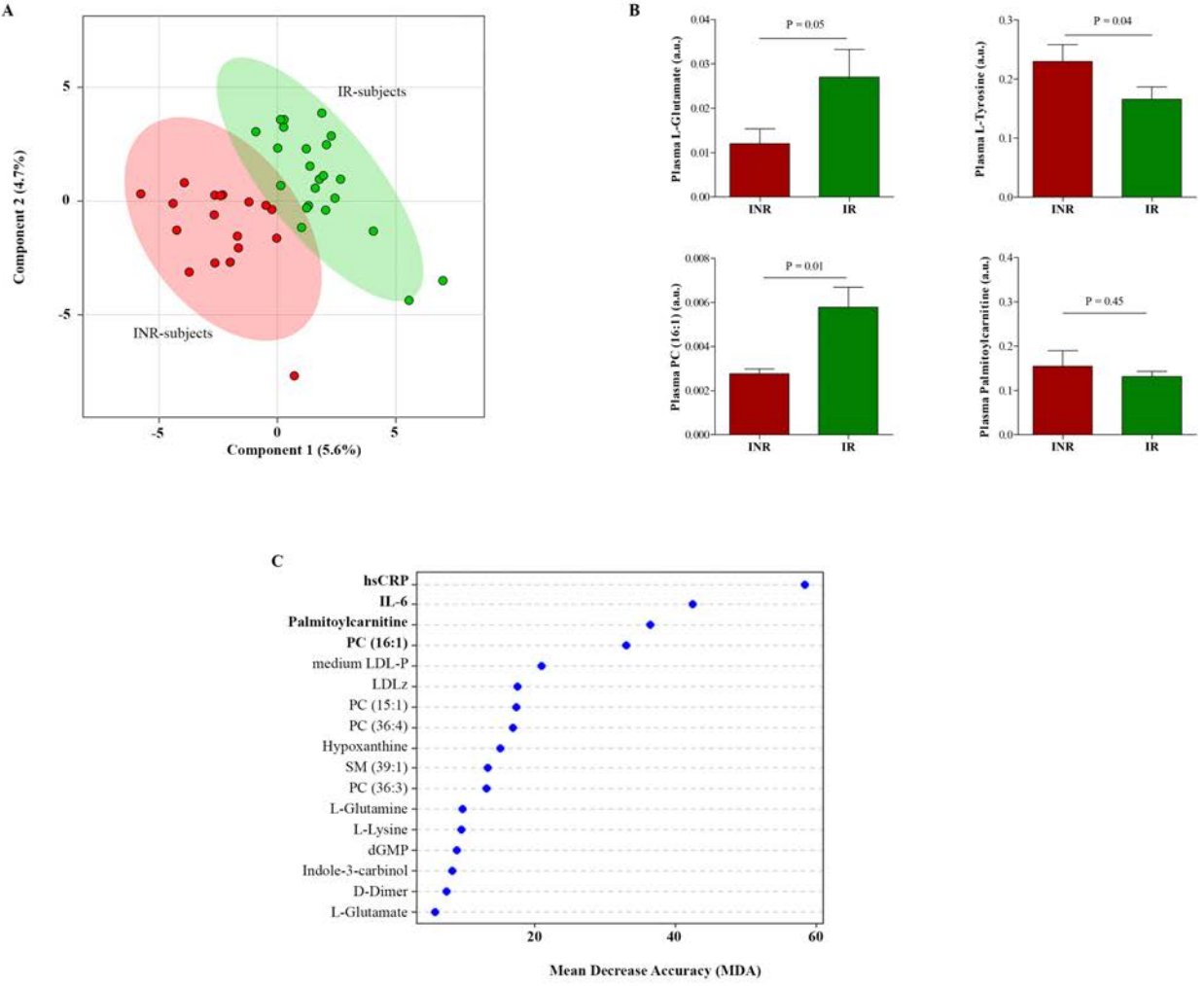
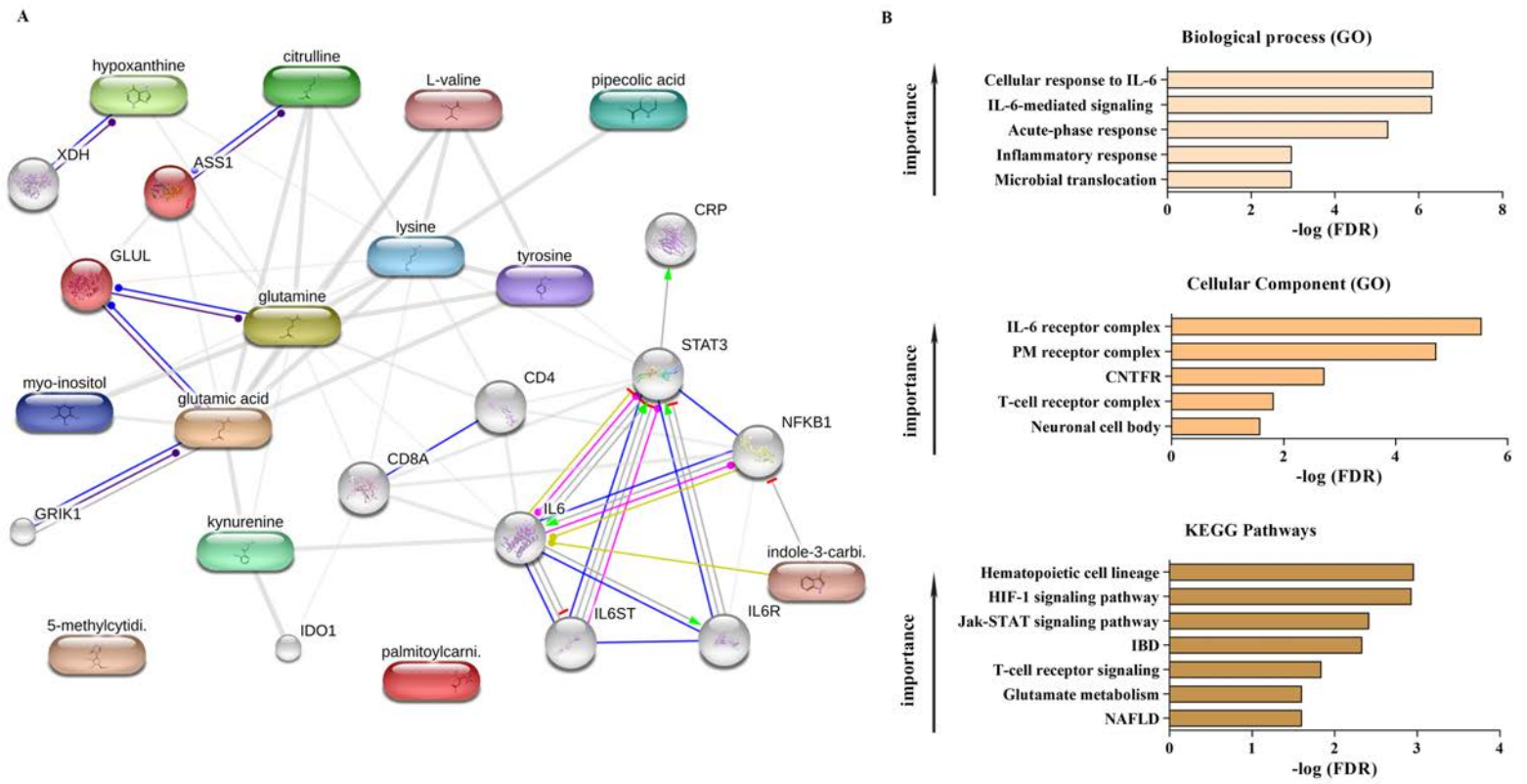


Figure 2



**Figure 3**

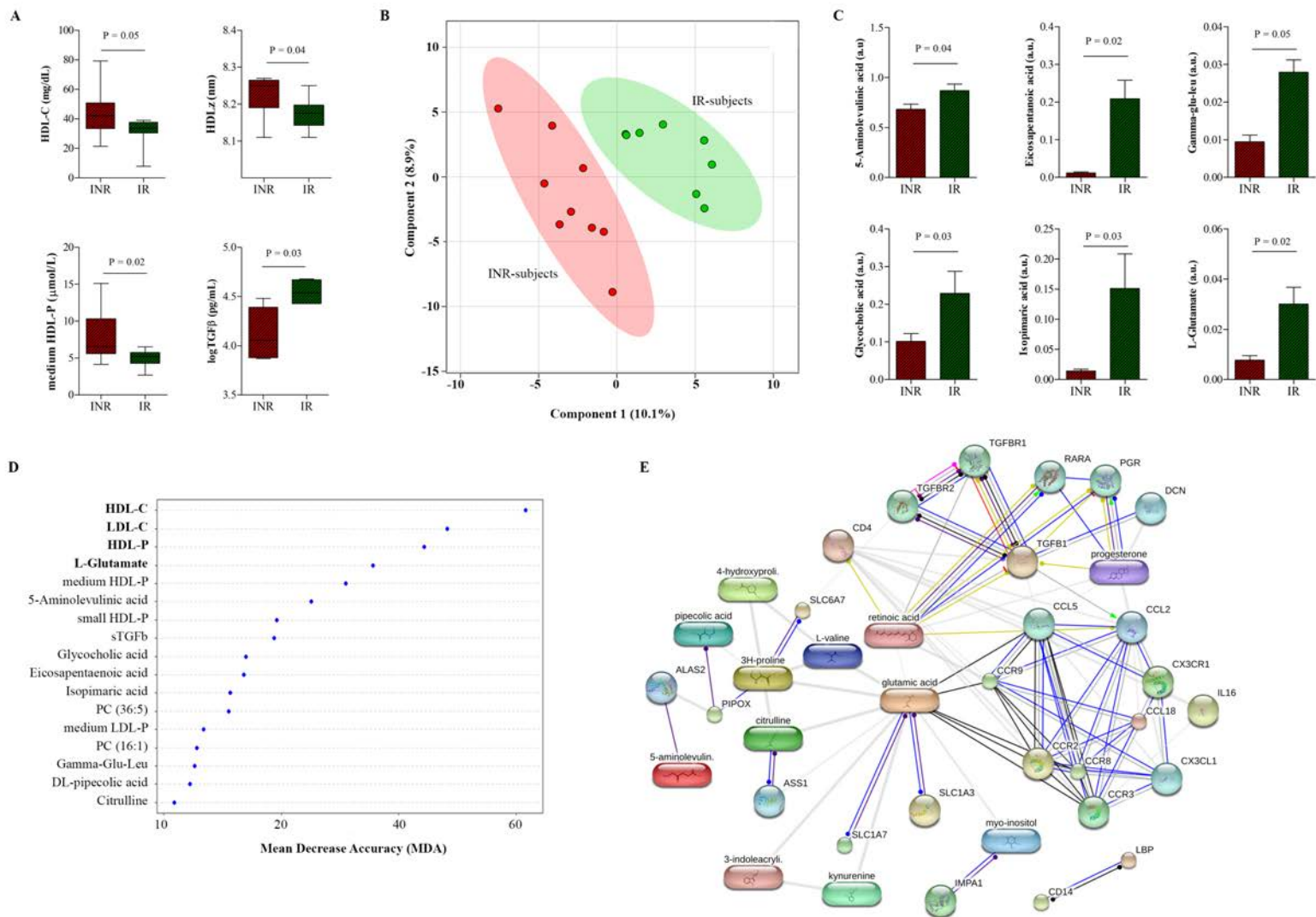
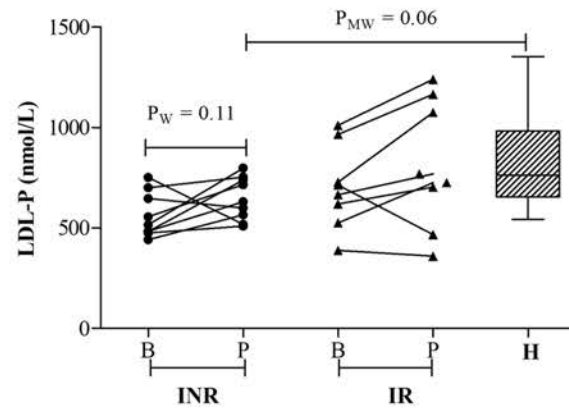
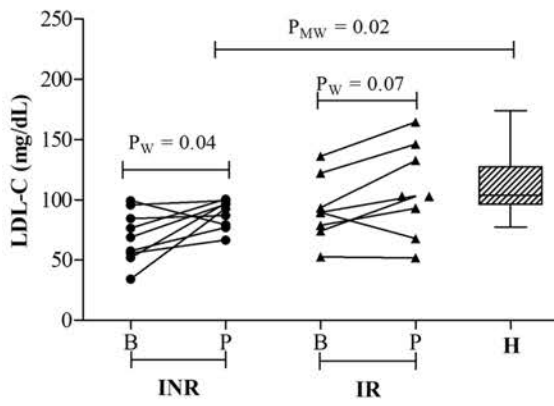


Figure 4

A



B

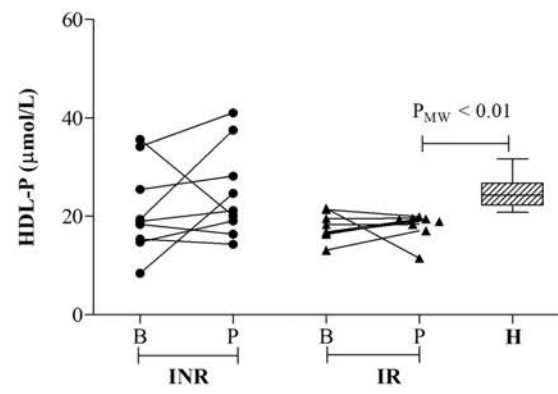
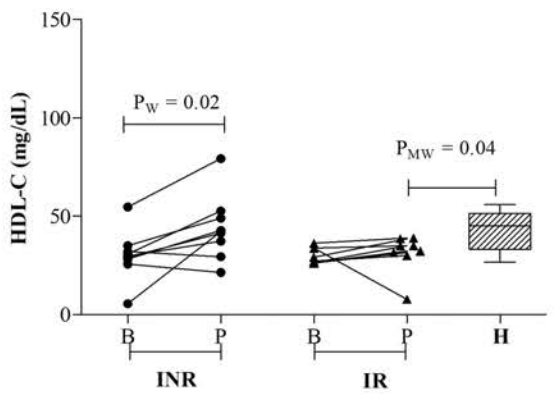
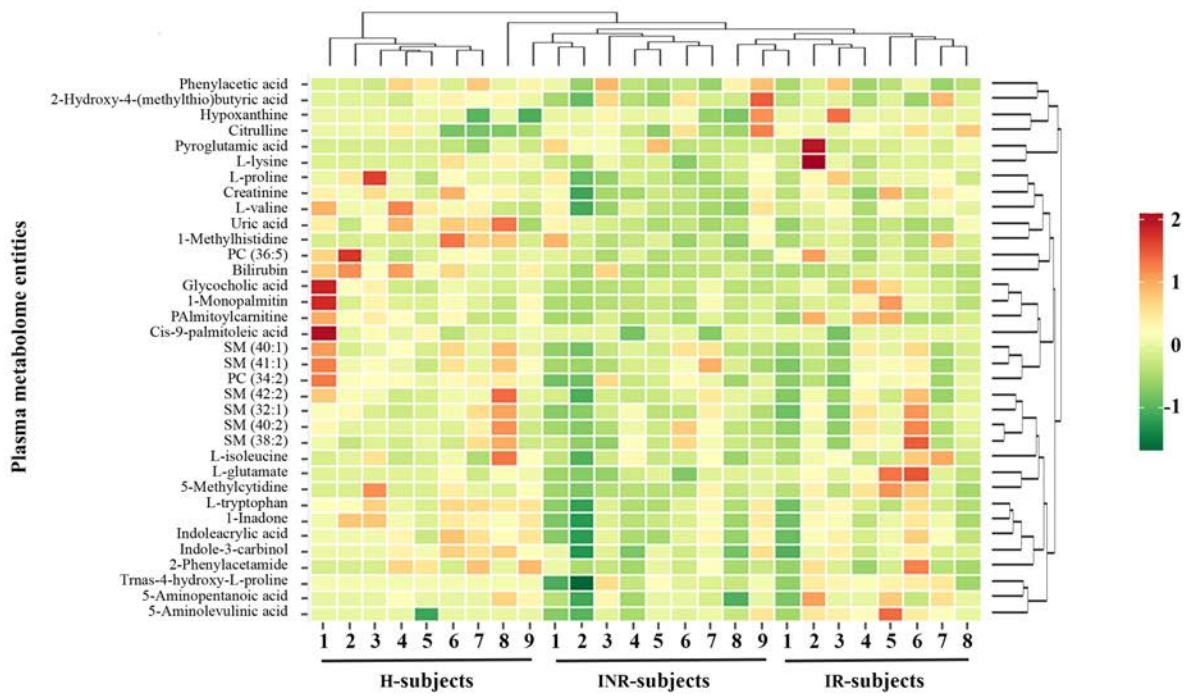


Figure 5



**Table 1.** Pre-cART characteristics of HIV-infected subjects.

	<b>All patients (n = 41)</b>	<b>INR subjects (n =18)</b>	<b>IR subjects (n=23)</b>	<b>P- value</b>
<b>Clinical characteristics</b>				
Age at cART initiation (years)	42 (34-51)	42 (33-55)	41 (33-49)	0.52
Risk factor				<b>0.03</b>
Heterosexual	11 (26.8)	8 (19.5)	3 (7.3)	
Homo/Bisexual	23 (56.1)	6 (14.6)	17 (41.5)	
Intravenous drug abuse	4 (9.8)	1 (2.4)	3 (7.3)	
Other	1 (2.4)	1 (2.4)	-	
Unknown	2 (4.9)	2 (4.9)	-	
CD4 T-cell count (cells/ $\mu$ L)	86 (63-161)	81 (44-143)	144 (74 -166)	0.17
CD8 T-cell count (cells/ $\mu$ L)	645 (574-1083)	598 (578-923)	889 (538-1642)	0.35
CD4/CD8 T-cell ratio	0.13 (0.08-0.26)	0.11 (0.07-0.27)	0.15 (0.10-0.25)	0.46
Plasma HIV RNA load (log copies/mL)	4.86 (4.42-5.32)	4.96 (4.13-5.29)	4.77 (4.54-5.32)	0.95
AIDS-related illness				0.34
Yes	10 (24.4)	5 (12.2)	5 (12.2)	
No	25 (61.0)	12 (29.3)	13 (31.7)	
Unknown	6 (14.6)	1 (2.4)	5 (12.2)	
HCV co-infection				0.41
Positive	3 (7.5)	2 (5.0)	1 (2.5)	
Negative	29 (72.5)	13 (32.5)	16 (40.0)	
Unknown	8 (20.0)	2 (5.0)	6 (15.0)	

Data are presented as n (%) or median (interquartile range). Categorical data were compared by means of a  $\chi^2$  test, whereas continuous data were compared using the Mann-Whitney test.

AIDS was diagnosed according to the CDC1993 criteria. P value < 0.05 was considered significant and is highlighted in bold.

## Supplement for

# Glutaminolysis and lipoproteins are key factors in late immune recovery in successfully treated HIV-infected patients

Isaac Rosado-Sánchez<sup>1±</sup>, Esther Rodríguez-Gallego<sup>2±</sup>, Joaquim Peraire<sup>2</sup>, Consuelo Viladés<sup>2</sup>, Pol Herrero<sup>3</sup>, Fran Fanjul<sup>4</sup>, Félix Gutiérrez<sup>5</sup>, Enrique Bernal<sup>6</sup>, Ricardo Pelazas<sup>7</sup>, Manuel Leal<sup>1,8</sup>, Sergi Veloso<sup>2</sup>, Miguel López-Dupla<sup>2</sup>, Julià Blanco<sup>9,10</sup>, Francesc Vidal<sup>2#\*</sup>, Yolanda María Pacheco<sup>1#\*</sup>, Anna Rull<sup>2#\*</sup>

<sup>1</sup> Laboratory of Immunology, Institute of Biomedicine of Seville, IBiS, UGC Clinical Laboratories, Virgen del Rocío University Hospital/CSIC/University of Seville, Seville, Spain

<sup>2</sup> Hospital Universitari Joan XXIII, IISPV, Universitat Rovira i Virgili, Tarragona, Spain

<sup>3</sup> Eurecat, Centre Tecnològic de Catalunya, Unitat de Ciències Òmiques (Unitat Mixta de Eurecat-Universitat Rovira i Virgili), Infraestructura Científico-Tècnica Singular (ICTS), Reus, Spain.

<sup>4</sup> Department of Infectious Diseases, Hospital Universitario Son Espases, Palma de Mallorca, Illes Balears, Spain

<sup>5</sup> Infectious Diseases Unit, Hospital General de Elche and Universidad Miguel Hernández, Alicante, Spain

<sup>6</sup> Department of Clinical Medicine, Universidad Católica San Antonio de Murcia and Hospital General Universitario Reina Sofía, Spain.

<sup>7</sup> Servicio de Medicina Interna, Hospital Universitario de Canarias, Universidad de La Laguna, Tenerife, Spain

<sup>8</sup> Internal Medicine Service, Viamed-Santa Ángela de la Cruz Hospital, Seville, Spain

<sup>9</sup> AIDS Research Institute IrsiCaixa, Institut Germans Trias I Pujol (IGTP); Universitat Autònoma de Barcelona, Badalona, Spain.

<sup>10</sup> Universitat de Vic-Universitat Central de Catalunya, Vic, Spain.

<sup>±</sup> Contributed equally to this work

<sup>#</sup> Senior authors that contributed equally to this work

**\*Correspondence to:** Francesc Vidal (fvidalmarsal.hj23.ics@gencat.cat), Yolanda M Pacheco (ypacheco-ibis@us.es), Anna Rull (anna.rull@iispv.cat)

**Table of Content:**

**Supplementary Table 1:** Selected soluble plasma biomarkers in cART-naïve HIV-infected subjects

**Supplementary Table 2:** Pre-cART NMR lipoprotein characteristics of study patients using Liposcale lipoprotein test.

**Supplementary Table 3:** Liposcale lipoprotein characterization of 17 HIV-infected subjects after 96 weeks of cART.

**Supplementary Table 4:** Soluble plasma biomarkers after 96 weeks of cART.

**Supplementary Table 5:** Plasma metabolome entities (n = 35) associated with disease progression in HIV infection.

**Supplementary Figure1:** Liposcale lipoprotein particle profile in a follow up subgroup of 9 INR and 8 IR compared to a group of healthy volunteers

**Supplementary Figure2:** Longitudinal evaluation of soluble plasma biomarkers.

**Supplementary Table 1:** Selected soluble plasma biomarkers in cART-naïve HIV-infected subjects

	<b>All patients (n = 34)</b>	<b>INR subjects (n =17)</b>	<b>IR subjects (n=17)</b>	<b>P- value</b>
<b>Soluble biomarkers</b>				
<b>Inflammation</b>				
IL-6 (pg/mL)	5.2 (3.4-8.6)	7.3 (3.6-12.5)	4.8 (2.9-6.2)	<b>0.03</b>
hsCRP (mg/L)	2.4 (0.8-6.1)	3.1 (0.8-9.4)	2.1 (0.8-3.7)	0.19
hsCRP ≥5 mg/L (%)	10 (29)	8 (48)	2 (11)	<b>0.02</b>
<b>Immune activation/suppression</b>				
IP-10 (pg/mL)	710.2 (322.7-1468.0)	573.4 (299.8-1624.0)	763.6 (506.9-1157.7)	0.93
log sCD14 (ng/mL)	3.5 (3.4-3.7)	3.5 (3.4-3.7)	3.5 (3.4-3.7)	0.76
log TGF-b (pg/mL)	4.3 (3.9-4.5)	4.2 (3.8-4.5)	4.3 (4.1-4.5)	0.50
<b>Microbial translocation</b>				
LPS (EU/mL)	0.2 (0.1-0.2)	0.2 (0.1-0.2)	0.2 (0.1-0.3)	0.18
<b>Endothelial dysfunction</b>				
sICAM-1 (ng/mL)	5.4 (5.2-5.5)	5.4 (5.2-5.5)	5.4 (5.2-5.5)	0.68
sVCAM-1 (ng/mL)	5.3 (5.4-5.7)	5.3 (5.4-5.7)	5.5 (5.4-5.6)	0.46
<b>Platelet activation</b>				
sCD40L (pg/mL)	145.1 (46.6-378.1)	110.4 (40.6-396.6)	149.3 (52.7-275.2)	0.90
<b>Coagulation</b>				
D-dimer (µg/L)	448 (260-916)	400 (253-866)	485 (251-1006)	0.44

Data are presented as median (interquartile range) and compared using the Mann-Whitney test.

All P values < 0.05 were considered significant and are highlighted in bold.

**Supplementary Table 2.** Pre-cART NMR lipoprotein characteristics of study patients using Liposcale test.

	<b>INR subjects (n=18)</b>	<b>IR subjects (n=23)</b>	<b>P-Value</b>
<b>Cholesterol concentration, mg/dL</b>			
VLDL-C	12.24 (9.62-19.37)	13.63 (11.95-18.31)	0.76
IDL-C	8.41 (6.01-10.23)	7.38 (11.95-18.31)	0.43
LDL-C	79.19 (65.98-91.96)	80.11 (65.54-93.49)	0.75
HDL-C	30.61 (28.79-35.64)	28.40 (26.18-33.87)	0.11
<b>Triglycerides concentration, mg/dL</b>			
VLDL-Tg	54.26 (39.18-78.59)	61.13 (42.20-69.01)	0.65
IDL-Tg	8.42 (6.39-11.33)	7.98 (5.58-9.38)	0.39
LDL-Tg	12.13 (8.19-16.91)	12.19 (5.49-16.18)	0.51
HDL-Tg	11.16 (10.36-14.31)	12.46 (8.84-13.84)	0.87
<b>Very low-density particle (VLDL-P) concentration, nmol/L</b>			
Total VLDL-P	32.28 (26.10-55.57)	41.80 (30.34-47.76)	0.56
Large VLDL-P	1.17 (0.79-1.56)	1.25 (0.74-1.53)	0.81
Medium VLDL-P	6.01 (4.58-8.12)	6.54 (4.81-7.30)	0.96
Small VLDL-P	27.73 (20.89-45.76)	32.94 (24.81-40.04)	0.55
<b>Low-density particle (LDL-P) concentration, nmol/L</b>			
Total LDL-P	564.56 (497.24-660.69)	594.61 (487.69-713.97)	0.79
Large LDL-P	73.05 (64.25-90.01)	76.66 (59.32-84.50)	0.83
Medium LDL-P	196.30 (180.48-237.15)	193.90 (139.69-266.70)	0.67
Small LDL-P	302.30 (253.82-335.89)	332.55 (267.25-373.28)	0.37
<b>High-density particle (HDL-P) concentration, <math>\mu</math>mol/L</b>			
Total HDL-P	18.91 (16.15-21.69)	17.81 (16.09-19.06)	0.29
Large HDL-P	0.09 (0.075-0.13)	0.07 (0.04-0.09)	<i>0.07</i>
Medium HDL-P	6.13 (5.30-6.83)	5.92 (5.08-6.40)	0.21
Small HDL-P	12.71 (10.09-15.07)	11.85 (10.73-13.44)	0.41
<b>Particle size, nm</b>			
VLDL z	42.83 (42.68-43.11)	42.85 (42.46-43.04)	0.43
LDL z	21.06 (20.93-21.16)	20.94 (20.90-21.10)	<i>0.09</i>
HDL z	8.22 (8.19-8.27)	8.22 (8.19-8.26)	0.70
<b>Others</b>			
Non- HDL particles, nmol/L	576.49 (547.21-682.74)	620.60 (514.42-745.12)	0.83
Total-P/HDL-P ratio	33.21 (24.84-39.64)	35.60 (30.75-42.63)	0.33
LDL-P/HDL-P ratio	31.31 (22.75-37.82)	33.33 (28.79-39.74)	0.43

Data are expressed as median (interquartile range).

Data were compared using the non-parametric Mann-Whitney U-test. All P values >0.05 but <0.15 were considered relevant for results interpretation and are italicized.

**Supplementary Table 3.** Liposcale lipoprotein characterization of 17 HIV-infected subjects after 96 weeks of cART.

	<b>INR subjects (n=9)</b>	<b>IR subjects (n=8)</b>	<b>P-Value</b>
<b>Cholesterol concentration, mg/dL</b>			
VLDL-C	16.46 (7.71-25.77)	20.21 (5.44-25.38)	0.85
IDL-C	7.40 (5.58-13.11)	7.26 (3.47-17.49)	0.92
LDL-C	92.79 (78.19-98.16)	102.97 (74.18-142.83)	0.15
HDL-C	42.14 (33.39-50.87)	33.65 (30.42-37.63)	<b>0.05</b>
<b>Triglycerides concentration, mg/dL</b>			
VLDL-Tg	55.81 (37.45-88.38)	60.87 (42.08-80.91)	0.70
IDL-Tg	8.46 (5.94-14.46)	9.35 (5.03-15.13)	1.00
LDL-Tg	14.97 (10.58-18.75)	12.62 (9.43-29.95)	0.88
HDL-Tg	12.18 (8.77-20.10)	9.45 (6.19-13.86)	0.23
<b>Very low-density particle (VLDL-P) concentration, nmol/L</b>			
Total VLDL-P	39.65 (24.01-59.59)	42.78 (27.11-57.83)	0.70
Large VLDL-P	1.20 (0.73-2.57)	1.48 (0.78-1.97)	0.92
Medium VLDL-P	6.38 (4.03-9.89)	7.66 (4.19-9.09)	0.57
Small VLDL-P	32.06 (19.21-47.13)	33.62 (21.72-46.77)	0.77
<b>Low-density particle (LDL-P) concentration, nmol/L</b>			
Total LDL-P	630.67 (541.98-745.88)	747.51 (526.44-1143.05)	0.34
Large LDL-P	91.29(77.13-98.10)	84.97 (73.66-154.87)	0.92
Medium LDL-P	259.10 (201.53-270.01)	267.96 (178.35-386.17)	0.44
Small LDL-P	296.19 (248.47-380.34)	408.34 (260.32-598.43)	0.25
<b>High-density particle (HDL-P) concentration, <math>\mu</math>mol/L</b>			
Total HDL-P	21.19 (17.73-32.85)	19.13 (17.39-19.58)	<i>0.08</i>
Large HDL-P	0.13 (0.06-0.16)	0.11 (0.09-0.12)	0.73
Medium HDL-P	6.55 (5.61-10.32)	5.20 (4.27-5.74)	<b>0.02</b>
Small HDL-P	14.78 (11.47-22.46)	13.73 (11.87-14.49)	0.25
<b>Particle size, nm</b>			
VLDL z	42.82 (42.68-42.89)	42.81 (42.62-43.02)	0.85
LDL z	21.13 (21.01-21.36)	20.99 (20.89-21.09)	0.10
HDL z	8.25 (8.19-8.26)	8.17 (8.14-8.19)	<b>0.04</b>
<b>Others</b>			
Non- HDL particles, nmol/L	629.13 (557.37-785.97)	752.73 (561.94-1214.63)	0.39
Total-P/HDL-P ratio	32.25 (22.06-36.03)	39.24 (30.50-71.59)	<i>0.08</i>
LDL-P/HDL-P ratio	29.92 (19.69-34.58)	38.07 (27.59-69.08)	<i>0.07</i>

Data are expressed as median values (interquartile range).

Values were compared using the non-parametric Mann-Whitney U-test. All P values < 0.05 were considered significant and are highlighted in bold. All P values >0.05 but <0.15 were considered relevant for results interpretation and are italicized.

**Supplementary Table 4:** Soluble plasma biomarkers after 96 weeks of cART.

	<b>INR subjects (n =6)</b>	<b>IR subjects (n=5)</b>	<b>P- value</b>
<b>Soluble biomarkers</b>			
<b>Inflammation</b>			
IL-6 (pg/mL)	4.16 (2.10-9.04)	4.03 (3.70-4.55)	1.00
hsCRP (mg/L)	1.30 (0.30-8.82)	0.70 (0.32-1.30)	0.28
<b>Immune activation/suppression</b>			
IP-10 (pg/mL)	177.05 (83.97-577.51) <sup>#</sup>	188.36 (91.04-280.37)	0.83
log sCD14 (ng/mL)	3.40 (3.33-3.86)	3.62 (3.54-3.79)	0.39
log TGF-b (pg/mL)	4.05 (3.87-4.39)	4.54 (4.43-4.67)	<b>0.03</b>
<b>Microbial translocation</b>			
LPS (EU/mL)	0.18 (0.09-0.21)	0.11 (0.08-0.13)	0.16
<b>Endothelial dysfunction</b>			
sICAM-1 (ng/mL)	5.23 (5.14-5.34)	5.24 (5.18-5.36)	0.91
sVCAM-1 (ng/mL)	5.50 (5.19-5.64)	5.32 (5.21-5.41)	0.52
<b>Platelet activation</b>			
sCD40L (pg/mL)	120.37 (13.79-258.35) <sup>#</sup>	236.65 (158.38-340.17)	0.29
<b>Coagulation</b>			
D-dimer (µg/L)	352 (162-801)	421 (254-577)	1.00

Data are presented as median (interquartile range) and compared using the Mann-Whitney test.

All P values < 0.05 were considered significant and are highlighted in bold.

**Supplementary Table 5.** Plasma metabolome entities (n = 35) associated with immune reconstitution in HIV infection.

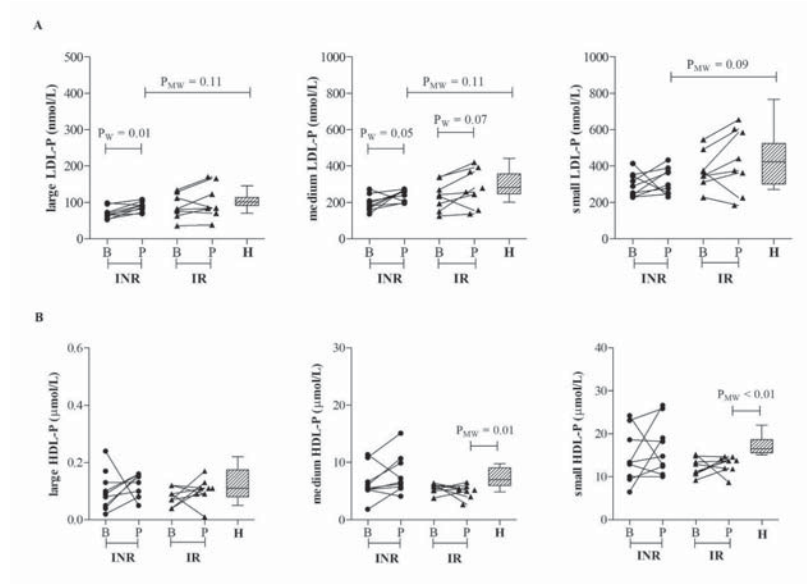
Compound	Reference	INR subjects (n = 9)		IR subjects (n = 8)		H-subjects (n = 9)
		Baseline	96 weeks	Baseline	96 weeks	
<i>P values &lt;0.05 in INR-subjects and IR-subjects at 96 weeks compared to H-subjects in the Mann-Whitney U-test</i>						
Bilirubin	HMDB0000054	0.024(0.016-0.052)	0.041(0.014-0.041)	0.021(0.011-0.077)	0.029(0.017-0.122)	0.314(0.197-0.498)
L-Tryptophan	HMDB0000929	0.785(0.049-1.077)	0.822(0.753-1.124)	0.854(0.611-0.984)	0.957(0.837-1.190)	1.321(1.115-1.395)
Uric acid	HMDB0000289	0.079(0.069-0.122)	0.081(0.066-0.119)	0.097(0.086-1.190)	0.075(0.060-1.024)	0.147(0.098-0.188)
SM (41:1)	SM(d16:1/25:0)	0.022(0.0181-0.030)	0.029(0.020-0.033)	0.027(0.016-0.038)	0.027(0.018-0.037)	0.038(0.033-0.050)
SM (40:1)	HMDB0012103	1.001(0.0677-0.121)	0.104(0.086-0.149)	0.109(0.075-0.157)	0.111(0.079-0.157)	0.129(0.122-0.193)
<i>P values &lt;0.05 in longitudinal evaluation of INR-subjects (Wilcoxon-test)</i>						
Phenylacetic acid	HMDB0000209	0.088(0.055-0.139)	0.122(0.068-0.302)	0.075(0.059-0.114)	0.104(0.071-0.184)	0.255(0.153-0.321)
Trans-4-Hydroxy-L-proline	HMDB0000725	0.279(0.185-0.331)	0.328(0.247-0.367)	0.321(0.247-0.389)	0.390(0.289-0.403)	-
SM(38:2)	SM(d16:1/22:1)	0.017(0.011-0.029)	0.027(0.019-0.042)	0.023(0.014-0.054)	0.036(0.019-0.046)	0.033(0.028-0.047)
SM(40:2)	HMDB11694	0.079(0.057-0.105)	0.096(0.079-0.143)	0.086(0.069-0.187)	0.127(0.068-0.168)	0.127(0.122-0.166)
<i>P values &lt;0.05 in longitudinal evaluation of IR-subjects (Wilcoxon-test)</i>						
2-hydroxy-4- (methylthio) butyric acid	HMDB0037115	0.082(0.041-0.138)	0.076(0.061-0.112)	0.049(0.041-0.061)	0.076(0.063-0.094)	0.092(0.085-0.101)
5(d)-Aminolevulinic Acid	HMDB0001149	0.638(0.616-0.921)	0.737(0.552-0.771)	0.737(0.619-0.916)	0.869(0.776-0.921)	0.367(0.367-0.367)
L-Isoleucine	HMDB0000172	0.474(0.280-0.510)	0.397(0.343-0.457)	0.344(0.277-0.412)	0.432(0.375-0.581)	0.453(0.391-0.549)
Pyroglutamic acid	HMDB0000267	0.071(0.051-0.087)	0.084(0.066-0.097)	0.074(0.068-0.095)	0.101(0.079-0.119)	0.111(0.083-0.132)

<i>P values &lt;0.05 in longitudinal evaluation of IR-subjects (Wilcoxon-test)</i>						
<i>P values &lt;0.05 in INR-subjects after 96 weeks of ART compared to healthy volunteers in the Mann-Whitney U-test</i>						
Creatinine	HMDB0000562	0.083(0.069-0.120)	0.094(0.091-0.122)	0.096(0.097-0.119)	0.129(0.101-0.155)	0.141(0.127-0.158)
Indoleacrylic acid	HMDB0000734	0.018(0.014-0.029)	0.021(0.019-0.030)	0.023(0.018-0.027)	0.031(0.023-0.033)	0.033(0.029-0.036)
<i>P values &lt;0.05 in longitudinal evaluation of IR-subjects (Wilcoxon-test)</i>						
<i>P values &lt;0.05 in INR-subjects and IR-subjects after 96 weeks of ART compared to healthy volunteers in the Mann-Whitney U-test</i>						
1-Indanone	HMDB0059602	0.041(0.033-0.060)	0.049(0.038-0.057)	0.047(0.034-0.051)	0.058(0.043-0.064)	0.068(0.068-0.076)
Indole-3-Carbinol	HMDB0005785	0.020(0.014-0.025)	0.024(0.017-0.027)	0.019(0.016-0.024)	0.025(0.024-0.031)	0.032(0.0291-0.035)
PC(34:2)	LMGP01010596	0.845(0.729-0.943)	0.890(0.670-1.018)	0.920(0.745-1.307)	0.878(0.689-1.031)	1.063(1.012-1.116)
<i>P values &lt;0.05 in INR-subjects after 96 weeks of ART compared to healthy volunteers in the Mann-Whitney U-test</i>						
1-Methylhistidine	HMDB0000001	0.016(0.013-0.039)	0.020(0.011-0.029)	0.025(0.017-0.031)	0.0189(0.014-0.030)	0.047(0.027-0.060)
1-Monopalmitin	HMDB0031074	0.025(0.0158-0.033)	0.019(0.013-0.029)	0.028(0.014-0.046)	0.033(0.019-0.065)	0.051(0.035-0.063)
2-Phenylacetamide	HMDB0010715	0.119(0.085-0.149)	0.108(0.072-0.148)	0.071(0.058-0.080)	0.087(0.056-0.229)	0.232(0.138-0.267)
5-Methylcytidine	HMDB0000982	0.017(0.015-0.020)	0.018(0.016-0.022)	0.026(0.014-0.033)	0.032(0.018-0.040)	0.029(0.024-0.040)
cis-9-palmitoleic acid	HMDB0003229	0.012(0.012-0.012)	0.057(0.020-0.057)	0.009(0.009-0.009)	0.020(0.020-0.020)	0.656(0.574-0.853)
Glycocholic Acid	HMDB0000138	0.119(0.060-0.178)	0.076(0.065-0.138)	0.152(0.093-0.252)	0.162(0.104-0.385)	0.208(0.136-0.312)
Hypoxanthine	HMDB0000157	0.280(0.039-1.439)	0.120(0.066-0.150)	0.089(0.057-0.120)	0.122(0.116-0.207)	0.031(0.028-0.031)
L-Glutamate	HMDB0000148	0.006(0.005-0.006)	0.006(0.004-0.011)	0.022(0.016-0.040)	0.023(0.017-0.045)	0.021(0.015-0.023)
L-Lysine	HMDB0000182	0.016(0.011-0.021)	0.012(0.009-0.014)	0.014(0.011-0.016)	0.014(0.011-0.024)	0.0190(0.016-0.023)
L-Proline	HMDB0000162	0.135(0.095-0.152)	0.133(0.101-0.171)	0.162(0.126-0.200)	0.175(0.141-0.205)	0.174(0.158-0.212)
L-Valine	HMDB0000883	0.197(0.166-0.447)	0.189(0.154-0.274)	0.219(0.209-0.282)	0.245(0.221-0.279)	0.271(0.237-0.356)

5-Aminopentanoic acid	HMDB0003355	0.035(0.031-0.035)	0.037(0.024-0.047)	0.036(0.031-0.045)	0.061(0.036-0.068)	0.055(0.049-0.061)
Palmitoylcarnitine	HMDB0000222	0.107(0.049-0.224)	0.081(0.056-0.115)	0.161(0.067-0.177)	0.121(0.059-0.308)	0.183(0.099-0.205)
PC(36:5)	C00157 (KEEG)	0.025(0.010-0.034)	0.017(0.011-0.024)	0.022(0.014-0.044)	0.029(0.0179-0.037)	0.032(0.026-0.050)
SM(32:1)	HMDB0012097	0.054(0.048-0.072)	0.067(0.052-0.072)	0.070(0.055-0.144)	0.094(0.050-0.123)	0.100(0.082-0.122)
SM(42:2)	HMDB0012107	0.288(0.179-0.432)	0.308(0.291-0.337)	0.307(0.232-0.489)	0.315(0.227-0.403)	0.364(0.328-0.437)
<i>P values &lt;0.05 in IR-subjects after 96weeks of ART compared to healthy volunteers in the Mann-Whitney U-test</i>						
Citrulline	HMDB0000904	0.010(0.007-0.013)	0.022(0.017-0.028)	0.026(0.011-0.028)	0.025(0.024-0.030)	0.014(0.014-0.022)

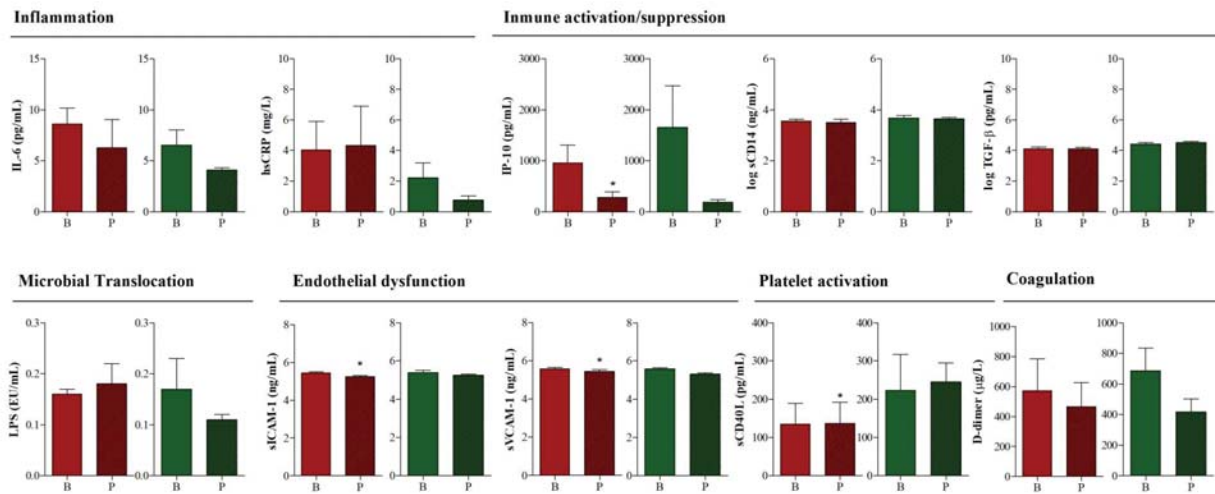
Data are expressed as median (IQR). HMDB was the abbreviation used for Human Metabolome Database (<http://www.hmdb.ca/>)

**Supplementary Figure1:** Liposcale lipoprotein particle profile in a follow up subgroup of 9 INR and 8 IR compared to a group of healthy volunteers.



(A) LDL particle subclasses were completely recovered in IR subjects achieving similar values of healthy subjects (H-subjects). (B) The number of HDL particles increased in HIV-infected subjects but remained lower in the subset of IR subjects compared to H-subjects. Comparisons between groups were performed with Mann-Whitney (MW) tests for unpaired samples and Wilcoxon t-test for paired samples (W). B was the abbreviation used for pre-cART values and P was the abbreviation used for values after 96 weeks of cART.

**Supplementary Figure2:** Longitudinal evaluation of soluble plasma biomarkers.



The introduction of cART clearly decreased inflammation (IL-6), immune activation (IP-10), endothelial dysfunction (ICAM-1, VCAM-1) and coagulation in all HIV-infected subjects, although differences were only significant for IP-10, ICAM-1 and VCAM-1 in INR subjects (red color). By contrast, microbial translocation was increased in INR subjects but decreased in IR subjects (green color) (not statistically significant). Comparisons between groups were performed using Wilcoxon t-test for paired samples (\*P<0.05 were considered significant). B was the abbreviation used for pre-cART values and P was the abbreviation used for values after 96 weeks of cART. Data are presented as mean ± SEM.